

# Moveout velocity analysis and parameter estimation for orthorhombic media

Vladimir Grechka and Ilya Tsvankin

*Center for Wave Phenomena, Colorado School of Mines*

## ABSTRACT

Orthorhombic symmetry describes several azimuthally anisotropic models typical for fractured formations, such as those containing two orthogonal crack systems or parallel vertical cracks in a VTI (transversely isotropic with a vertical symmetry axis) background. Here, we present a methodology to invert multi-azimuth  $P$ -wave reflection traveltimes for the parameters of vertically inhomogeneous orthorhombic media. Our approach is based on the general analytic representation of normal-moveout (NMO) velocity as an ellipse in the horizontal plane. A minimum of three differently oriented common-midpoint (CMP) lines is sufficient to reconstruct the ellipse and obtain normal-moveout velocity in any azimuthal direction. Then the orientation and the semi-axes of the NMO ellipse, which are dependent on both anisotropy and heterogeneity, can be inverted for the medium parameters.

Our analytic and numerical study shows that for the model of a homogeneous orthorhombic layer above a dipping reflector, the exact  $P$ -wave NMO velocity is determined by *five* parameters – the normal-moveout velocities from a horizontal reflector measured in the symmetry planes  $[V_{\text{nmo}}^{(1,2)}]$  and three anisotropic coefficients  $\eta^{(1,2,3)}$  introduced by analogy with the Alkhalifah-Tsvankin parameter  $\eta$  for VTI media. The velocities  $V_{\text{nmo}}^{(1,2)}$  and the orientation of the vertical symmetry planes can be found using the azimuthally dependent NMO velocity from a horizontal reflector. Then the NMO ellipse of at least one dipping event is needed to obtain the coefficients  $\eta^{(1,2,3)}$  that control the dip dependence of normal moveout. We discuss the stability of the inversion procedure and specify the constraints on the dip and azimuth of the reflector; for instance, for all three  $\eta$  coefficients to be resolved individually, the dip plane of the reflector should not coincide with either of the symmetry planes.

To carry out parameter estimation in vertically inhomogeneous orthorhombic media, we apply the generalized Dix equation that operates with the matrices responsible for interval NMO ellipses (rather with the normal-moveout velocities themselves). Our algorithm is designed to find the interval values of  $V_{\text{nmo}}^{(1,2)}$  and  $\eta^{(1,2,3)}$  using moveout from horizontal and dipping reflectors measured at different vertical times. Application to a synthetic multi-azimuth  $P$ -wave data set over a layered orthorhombic medium with depth-varying orientation of the symmetry planes verifies the accuracy of the inversion method.

## Introduction

Reflection moveout and, in particular, normal-moveout (NMO) velocity have been extensively used to build isotropic velocity models of the subsurface (e.g., Hubral and Krey, 1980). The main complication in extending these velocity-analysis methods to anisotropic media is

the multi-parameter nature of the problem: the angular dependence of the velocity function at each spatial location is described by several (up to 21) elastic coefficients. Even for relatively simple transversely isotropic (TI) media,  $P$ - and  $SV$ -wave propagation (the qualifiers in “quasi- $P$ -wave” and “quasi- $S$ -wave” will be omitted) is governed by the orientation of the symmetry axis and

four stiffness coefficients. This number, however, can be reduced if we focus exclusively on kinematic signatures of  $P$ -waves that depend (for a fixed symmetry-axis orientation), on just the symmetry-direction velocity  $V_{P0}$  and Thomsen's anisotropic coefficients  $\epsilon$  and  $\delta$  (Tsvankin and Thomsen, 1994). Furthermore, as shown by Alkhalifah and Tsvankin (1995),  $P$ -wave NMO velocity and all *time*-processing steps [NMO and dip-moveout (DMO) correction, time migration] in TI models with a vertical symmetry axis (VTI media) are controlled by only two combinations of  $V_{P0}$ ,  $\epsilon$  and  $\delta$  – the zero-dip NMO velocity  $V_{\text{nmo}}(0)$  and the “anellipticity” coefficient  $\eta$ . Alkhalifah and Tsvankin also developed a method for obtaining  $V_{\text{nmo}}(0)$  and  $\eta$  in vertically inhomogeneous VTI media using  $P$ -wave NMO velocities from two different dips (e.g., from horizontal and dipping interfaces). This algorithm, however, is based on the 2-D NMO equation of Tsvankin (1995) that can be applied only to common-midpoint (CMP) lines in the dip plane of the reflector.

Reflection moveout for out-of-plane (3-D) wave propagation in inhomogeneous anisotropic media was described by Grechka and Tsvankin (1996) who showed that the azimuthal dependence of NMO velocity typically represents an *ellipse* in the horizontal plane. In the special case of a single layer with a horizontal symmetry plane, the elliptical dependence of NMO velocity was obtained by Sayers (1995) who developed an approximate representation of long-spread moveout based on an expansion of group velocity in spherical harmonics. If the medium above the reflector has the VTI symmetry, the axes of the ellipse lie in the dip and strike directions of the reflector. Grechka and Tsvankin (1996) proved that *both* semi-axes of the  $P$ -wave NMO ellipse (and, therefore, the NMO velocity in any azimuthal direction) for VTI media depend on the two Alkhalifah-Tsvankin parameters,  $V_{\text{nmo}}(0)$  and  $\eta$ . NMO velocity and zero-offset traveltimes for a dipping event obtained on two CMP lines with different azimuthal orientation are needed to recover  $V_{\text{nmo}}(0)$  and  $\eta$ , along with the unknown reflector azimuth. Alternatively, both parameters can be found using normal moveout from a horizontal and dipping reflectors on a single CMP line with arbitrary azimuthal orientation (Grechka and Tsvankin, 1996). Additional azimuths, if available, provide redundant information that might increase the accuracy of the parameter estimation.

In this paper, we use the analytic results of Grechka and Tsvankin (1996) and Grechka et al. (1997) to generalize this methodology for more complicated, azimuthally anisotropic media. The NMO ellipse for a given reflection event in any anisotropic model is still described by three independent parameters (e.g., the two semi-axes and the azimuth of one of them) and can be reconstructed from

NMO velocities measured in at least three different azimuthal directions. Then the parameters of the ellipse can be inverted for the combinations of the medium coefficients responsible for normal moveout of the  $P$ -wave or some other recorded mode. In general, this inversion requires moveout data for several reflectors with different dips and azimuths (depending on the symmetry of the medium).

Although conceptually this problem can be solved for arbitrary anisotropic media, this work is restricted to orthorhombic (or orthotropic) anisotropy that describes several models typical for fractured reservoirs (e.g., Wild and Crampin, 1991; Schoenberg and Helbig, 1997; Tsvankin, 1996b). For instance, orthorhombic symmetry may be caused by a system of parallel vertical cracks embedded in a background VTI medium (Figure 1) and two orthogonal (or non-orthogonal but *identical*) vertical crack systems in a purely isotropic or VTI matrix. Although orthorhombic models are described by nine independent stiffness coefficients,  $P$ -wave velocities and traveltimes depend on just the vertical velocity and five anisotropic coefficients introduced by Tsvankin (1996b). Grechka and Tsvankin (1996) provided exact explicit expressions for NMO velocity in a horizontal orthorhombic layer and demonstrated that Tsvankin's notation (briefly reviewed below) leads to a significant simplification in the analytic description of NMO velocity.

Extending this result to a homogeneous orthorhombic layer above a *dipping* reflector, we show that  $P$ -wave normal-moveout velocity (expressed through the horizontal slowness components of the zero-offset ray) depends on the NMO velocities from a horizontal reflector in the symmetry planes [ $V_{\text{nmo}}^{(1,2)}$ ] and three anisotropic parameters  $\eta^{(1,2,3)}$  defined similarly to the Alkhalifah-Tsvankin coefficient  $\eta$ . This conclusion is in agreement with the work by Ikelle (1996) who showed that the dispersion relation in weakly anisotropic orthorhombic media depends on the two zero-dip NMO velocities in the symmetry planes and three “anellipticity” coefficients. All five parameters can be obtained from surface  $P$ -wave data using azimuthally-dependent NMO velocity from a horizontal and at least one dipping interface (provided the dip plane of the reflector is not too close to either of the vertical symmetry planes) or, alternatively, using two different dipping events. To find the interval values of  $V_{\text{nmo}}^{(1,2)}$  and  $\eta^{(1,2,3)}$  in *horizontally-layered* orthorhombic media above a dipping reflector, we devise a layer-stripping procedure based on the generalized Dix equation of Grechka et al. (1997). Finally, we apply our inversion algorithm to synthetic  $P$ -wave traveltimes generated by ray tracing for a stratified orthorhombic

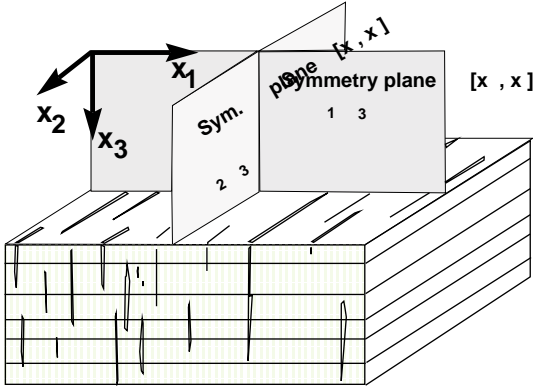


**Figure 1.** Orthorhombic media have three mutually orthogonal planes of mirror symmetry. One of the reasons for orthorhombic anisotropy is a combination of parallel vertical cracks and vertical transverse isotropy (e.g., due to thin horizontal layering) in the background medium.

model with a different orientation of the vertical symmetry planes in each layer.

### Notation for Orthorhombic Media

Orthorhombic (or orthotropic) media have three mutually orthogonal planes of mirror symmetry; for the model with a single system of vertical cracks in a VTI background (Figure 1), the symmetry planes are determined by the crack orientation. Here, we assume that one of the symmetry planes is horizontal, but we do not restrict ourselves to any particular physical model and consider the general stiffness tensor for orthorhombic media that has nine independent components  $c_{ij}$ . Evidently, inverting moveout information for nine (generally spatially varying) parameters is an extremely difficult problem, especially given a limited angle coverage of reflection data.

Significant progress, however, can be made by combining the stiffnesses in such a way that will simplify analytic description of seismic velocities and amplitudes. Tsvankin (1996b) used the identical form of the Christoffel equation in the symmetry planes of orthorhombic and TI media to introduce a notation based on the same principle as Thomsen (1986) parameters for vertical transverse isotropy. Tsvankin's notation contains two "isotropic" quantities (the vertical velocities of the  $P$ -wave and one of the split  $S$ -waves) and seven dimensionless anisotropic parameters similar to the VTI coefficients  $\epsilon$ ,  $\delta$  and  $\gamma$ . The definitions of these parameters and their brief description are as follows:

- $V_{P0}$  –  $P$ -wave vertical velocity:

$$V_{P0} \equiv \sqrt{\frac{c_{33}}{\rho}} \quad (\rho \text{ is the density}). \quad (1)$$

- $V_{S0}$  – the vertical velocity of the  $S$ -wave polarized in the  $x_1$ -direction:

$$V_{S0} \equiv \sqrt{\frac{c_{55}}{\rho}}. \quad (2)$$

- $\epsilon^{(2)}$  – the VTI parameter  $\epsilon$  in the  $[x_1, x_3]$  symmetry plane normal to  $x_2$ -axis (this explains the superscript "2"):

$$\epsilon^{(2)} \equiv \frac{c_{11} - c_{33}}{2 c_{33}}. \quad (3)$$

- $\delta^{(2)}$  – the VTI parameter  $\delta$  in the  $[x_1, x_3]$  plane:

$$\delta^{(2)} \equiv \frac{(c_{13} + c_{55})^2 - (c_{33} - c_{55})^2}{2 c_{33} (c_{33} - c_{55})}. \quad (4)$$

- $\gamma^{(2)}$  – the VTI parameter  $\gamma$  in the  $[x_1, x_3]$  plane :

$$\gamma^{(2)} \equiv \frac{c_{66} - c_{44}}{2 c_{44}}. \quad (5)$$

- $\epsilon^{(1)}$  – the VTI parameter  $\epsilon$  in the  $[x_2, x_3]$  symmetry plane:

$$\epsilon^{(1)} \equiv \frac{c_{22} - c_{33}}{2 c_{33}}. \quad (6)$$

- $\delta^{(1)}$  – the VTI parameter  $\delta$  in the  $[x_2, x_3]$  plane:

$$\delta^{(1)} \equiv \frac{(c_{23} + c_{44})^2 - (c_{33} - c_{44})^2}{2 c_{33} (c_{33} - c_{44})}. \quad (7)$$

- $\gamma^{(1)}$  – the VTI parameter  $\gamma$  in the  $[x_2, x_3]$  plane:

$$\gamma^{(1)} \equiv \frac{c_{66} - c_{55}}{2 c_{55}}. \quad (8)$$

- $\delta^{(3)}$  – the VTI parameter  $\delta$  in the  $[x_1, x_2]$  plane ( $x_1$  plays the role of the symmetry axis):

$$\delta^{(3)} \equiv \frac{(c_{12} + c_{66})^2 - (c_{11} - c_{66})^2}{2 c_{11} (c_{11} - c_{66})}. \quad (9)$$

This notation preserves the attractive features of Thomsen parameters (discussed in detail by Tsvankin, 1996a) in describing symmetry-plane velocities, traveltimes and reflection coefficients. Also, as shown by Tsvankin (1996b), a subset of the parameters introduced above captures the combinations of  $c_{ij}$ 's responsible for  $P$ -wave kinematic signatures both within and *outside* symmetry planes, even for strongly anisotropic orthorhombic media.  $P$ -wave velocities and traveltimes (including reflection moveout) depend on just *six* parameters ( $V_{P0}$ ,  $\epsilon^{(1)}$ ,  $\delta^{(1)}$ ,  $\epsilon^{(2)}$ ,  $\delta^{(2)}$ , and  $\delta^{(3)}$ ) and the orientation of the symmetry planes, rather than nine coefficients in the conventional  $c_{ij}$  notation. Since the parameters  $\delta^{(1)}$  and  $\delta^{(2)}$  determine near-vertical  $P$ -wave velocity variations, they concisely describe  $P$ -wave NMO velocity from horizontal reflectors (Grechka and Tsvankin, 1996).

The results below show that *dip-dependent* normal moveout is a function of simple combinations of  $\epsilon$ 's and  $\delta$ 's as well.

Another advantage of this notation is the convenience of characterizing anisotropy by a set of dimensionless anisotropic coefficients which go to zero in isotropic media and are well-suited for developing weak-anisotropy approximations for various seismic signatures. Below, we will apply the weak-anisotropy approximation to the NMO-velocity function to identify the parameters that govern  $P$ -wave moveout in orthorhombic media.

### Equation of the NMO Ellipse

Grechka and Tsvankin (1996) considered azimuthally dependent reflection moveout of pure (non-converted) modes around a certain common-midpoint (CMP) location over arbitrary anisotropic inhomogeneous media. By expanding the one-way traveltime  $\tau$  from the zero-offset reflection point to the surface into a double Taylor series with respect to the horizontal Cartesian coordinates  $(x_1, x_2)$ , they derived the following expression for the normal-moveout velocity  $V_{\text{nmo}}$  (see also Grechka et al., 1997):

$$V_{\text{nmo}}^{-2}(\alpha) = W_{11} \cos^2 \alpha + 2W_{12} \sin \alpha \cos \alpha + W_{22} \sin^2 \alpha, \quad (10)$$

where  $\alpha$  is the azimuth of the CMP line with respect to the  $x_1$ -axis, and the symmetric matrix  $\mathbf{W}$  is given by

$$W_{ij} = \tau_0 \left. \frac{\partial^2 \tau}{\partial x_i \partial x_j} \right|_{\tau=\tau_0} = \tau_0 \frac{\partial p_i}{\partial x_j}, \quad (i, j = 1, 2). \quad (11)$$

Here,  $\tau_0$  is the one-way zero-offset traveltime and  $p_1$  and  $p_2$  are the horizontal components of the slowness vector; the spatial derivatives of  $\tau$  and  $p_i$  are evaluated for the zero-offset ray (i.e., at the CMP location). Grechka and Tsvankin (1996) showed that if the CMP traveltime increases with offset for all azimuths  $\alpha$  (which is usually the case), the matrix  $\mathbf{W}$  is positive definite and the azimuthally varying NMO velocity (10) represents an *ellipse*. To demonstrate the elliptical character of  $V_{\text{nmo}}(\alpha)$ , equation (10) can be rewritten as (for details see Grechka and Tsvankin, 1996 and Grechka et al., 1997)

$$V_{\text{nmo}}^{-2}(\alpha) = \lambda_1 \cos^2(\alpha - \beta) + \lambda_2 \sin^2(\alpha - \beta), \quad (12)$$

where  $\lambda_{1,2}$  are the eigenvalues of the matrix  $\mathbf{W}$ , and  $\beta$  is the rotation angle (determined by the eigenvectors of  $\mathbf{W}$ ) defined as

$$\beta = \tan^{-1} \left[ \frac{W_{22} - W_{11} + \sqrt{(W_{22} - W_{11})^2 + 4W_{12}^2}}{2W_{12}} \right]. \quad (13)$$

Except for uncommon models with reverse moveout (i.e., with negative  $V_{\text{nmo}}^2$ , which implies that  $\lambda_1 < 0$  and/or  $\lambda_2 < 0$ ) equation (12) does indeed describe an ellipse in the horizontal plane (Grechka and Tsvankin, 1996). The NMO velocities in the directions of the elliptical axes (we denote them  $v_{e\ell 1}$  and  $v_{e\ell 2}$ ) are expressed through the eigenvalues as  $v_{e\ell 1} = 1/\sqrt{\lambda_1}$  and  $v_{e\ell 2} = 1/\sqrt{\lambda_2}$ .

Since the NMO ellipse (10) is fully defined by only three quantities ( $W_{11}$ ,  $W_{12}$ , and  $W_{22}$ ), it can be reconstructed from reflection data using a minimum of three NMO-velocity measurements in different azimuthal directions. Below, we show how the elements of the matrix  $\mathbf{W}$  for horizontal and dipping events can be inverted for the parameters of orthorhombic media.

### Normal-moveout Velocity in a Homogeneous Orthorhombic Layer

#### Horizontal layer

As mentioned above, we consider an orthorhombic medium with a horizontal symmetry plane. Then the other two (vertical) symmetry planes determine the orientation of the NMO ellipse in a horizontal orthorhombic layer. Indeed, aligning the coordinate directions  $x_1$  and  $x_2$  with the vertical symmetry planes, we find that  $W_{12} = 0$ , and equation (10) reduces to (Grechka and Tsvankin, 1996)

$$V_{\text{nmo}}^{-2}(\alpha, 0) = W_{11} \cos^2 \alpha + W_{22} \sin^2 \alpha \quad (14)$$

$$= [V_{\text{nmo}}^{(2)}]^{-2} \cos^2 \alpha + [V_{\text{nmo}}^{(1)}]^{-2} \sin^2 \alpha,$$

where  $V_{\text{nmo}}^{(2)}$  and  $V_{\text{nmo}}^{(1)}$  are the NMO velocities in the symmetry planes that can be easily found by analogy with vertical transverse isotropy (Tsvankin, 1996b). For instance, the symmetry-plane NMO velocities for  $P$ -waves are given by

$$V_{\text{nmo}}^{(i)} = V_{P0} \sqrt{1 + 2\delta^{(i)}}, \quad (i = 1, 2), \quad (15)$$

where  $V_{P0}$  and  $\delta^{(i)}$  are introduced in equations (1), (4), and (7). The remarkable simplicity of the exact NMO equations (14) and (15) illustrates the advantages of Tsvankin's parameterization (1) – (9).

Clearly, by obtaining the  $P$ -wave NMO ellipse in a horizontal orthorhombic layer, we can determine the orientation of the vertical symmetry planes and the NMO velocities  $V_{\text{nmo}}^{(1,2)}$  within them. The only case in which the azimuths of the symmetry planes cannot be resolved is when the ellipse degenerates into a circle (i.e.,  $V_{\text{nmo}}^{(2)} = V_{\text{nmo}}^{(1)}$ ). Likewise, the symmetry-plane directions can be recovered from the azimuthally-dependent NMO velocities of either split shear mode.

### Layer above a dipping reflector

#### NMO equation for general anisotropy

If the bottom of a homogeneous orthorhombic layer is *dipping*, the azimuthal dependence of normal-moveout velocity is influenced by both the reflector orientation and azimuthal anisotropy. Unless the dip plane of the reflector coincides with one of the symmetry planes of the medium, the model as a whole does not have vertical symmetry planes, and NMO velocity can no longer be described by equation (14). While the azimuthal variation of normal-moveout velocity remains elliptical in accordance with the general equation (10), the semi-axes of the NMO ellipse do not necessarily coincide with the symmetry-plane directions of the layer above the reflector.

For the purposes of traveltime inversion, it is essential to express the NMO velocity through quantities that can be measured from reflection data. In the 2-D problem dealing with moveout in the dip plane of the reflector (that should coincide with a symmetry plane of the medium), the slope of reflections on the zero-offset section yields the ray parameter (horizontal slowness) of the zero-offset ray (Alkhalifah and Tsvankin, 1995). (Recovering the actual dip of the reflector from reflection traveltimes requires knowledge of the velocity field, even if the medium is purely isotropic.) Similarly, in the more general 3-D case discussed here, the horizontal components ( $p_1$  and  $p_2$ ) of the zero-offset slowness vector can be obtained directly from the azimuthally dependent slope of zero-offset reflections. Although we do need a minimum of three different azimuths to reconstruct the NMO ellipse, the zero-offset sections along any *two* of them can be used to find  $p_1$  and  $p_2$  (Grechka and Tsvankin, 1996). Indeed, the zero-offset reflection slope in any azimuthal direction is simply equal to the projection of the zero-offset slowness vector onto this direction. Snell's law implies that the slowness vector of the zero-offset ray (but not necessarily the ray itself) is normal to the reflector at the zero-offset reflection point. The components  $p_1$  and  $p_2$ , therefore, allow us to determine the reflector *azimuth*, while the *dip* still remains unknown because the vertical slowness component cannot be found directly from traveltimes measured in the horizontal plane.

The analysis below is based on the exact explicit expression for NMO velocity in a homogeneous layer of arbitrary symmetry given by Grechka et al. (1997), who expressed the components of the matrix  $\mathbf{W}$  through the slowness vector of the zero-offset ray:

$$\mathbf{W} = \frac{p_1 q_{,1} + p_2 q_{,2} - q}{q_{,11} q_{,22} - q_{,12}^2} \begin{pmatrix} q_{,22} & -q_{,12} \\ -q_{,12} & q_{,11} \end{pmatrix}, \quad (16)$$

where  $q \equiv q(p_1, p_2) \equiv p_3$  is the vertical component of the slowness vector;  $q_{,i}$  and  $q_{,ij}$ , ( $i, j=1,2$ ) denote the partial derivatives  $q_{,i} \equiv \partial q / \partial p_i$  and  $q_{,ij} \equiv \partial^2 q / \partial p_i \partial p_j$  that should be evaluated for the zero-offset ray. Substitution of  $\mathbf{W}$  into equation (10) for the NMO ellipse yields

$$V_{\text{nmo}}^{-2}(\alpha, p_1, p_2) = \frac{p_1 q_{,1} + p_2 q_{,2} - q}{q_{,11} q_{,22} - q_{,12}^2} \left[ q_{,22} \cos^2 \alpha - 2 q_{,12} \sin \alpha \cos \alpha + q_{,11} \sin^2 \alpha \right], \quad (17)$$

Equation (18) is valid for all pure (non-converted) reflection modes and any mutual orientation of the CMP line and reflector strike. The vertical slowness  $q \equiv p_3$  can be found from the Christoffel equation,

$$\det(c_{ijkl} p_j p_k - \rho \delta_{il}) = 0, \quad (18)$$

where  $\delta_{il}$  is the Kronecker's symbolic delta. Then the derivatives  $q_{,i}$  and  $q_{,ij}$  can be calculated by implicit differentiation of equation (18), as suggested by Grechka et al. (1997).

Although the NMO equation (18) is quite general, here we will apply it only to  $P$ -waves in orthorhombic media. Since the NMO ellipse (18) is defined by three components of the matrix  $\mathbf{W}$  (i.e., three coefficients of the trigonometric functions), no more than three combinations of the layer parameters can be extracted from moveout measurements for a single reflector with certain values of  $p_1$  and  $p_2$ . As discussed above, if the reflector is horizontal,  $P$ -wave NMO velocity is sufficient to determine the orientation of the symmetry planes and the NMO velocities within them. An important question addressed below is which parameters of an orthorhombic medium can be obtained using  $P$ -wave NMO velocity from dipping reflectors with different strike orientation.

#### $P$ -wave NMO velocity in the weak-anisotropy limit

Although numerical evaluation of equation (18) is relatively straightforward, the dependence of NMO velocity on the medium parameters is hidden in the vertical slowness component and its derivatives. Therefore, to identify the coefficients responsible for  $P$ -wave NMO velocity, it is convenient to apply the weak-anisotropy approximation. This approach has proved extremely productive in the analysis of NMO velocity and other seismic signatures for vertical transverse isotropy (Tsvankin, 1995, 1996a; Alkhalifah and Tsvankin, 1995). For instance, Alkhalifah and Tsvankin (1995) provided analytic support for their two-parameter methodology by showing that  $P$ -wave NMO velocity in weakly anisotropic VTI media depends just on the zero-dip value  $V_{\text{nmo}}(0)$  and the difference  $\epsilon - \delta \approx \eta$ .

To express the vertical slowness through  $p_1$  and  $p_2$ , we use the  $P$ -wave phase-velocity equation for weakly

orthorhombic media given in Tsvankin (1996b):

$$V^2 = V_{P0}^2 [1 + 2n_1^4 \epsilon^{(2)} + 2n_2^4 \epsilon^{(1)} + 2n_1^2 n_3^2 \delta^{(2)} + 2n_2^2 n_3^2 \delta^{(1)} + 2n_1^2 n_2^2 (2\epsilon^{(2)} + \delta^{(3)})]. \quad (19)$$

Here  $\mathbf{n} = \mathbf{p}V$  is the unit vector in the slowness direction ( $\mathbf{p}$  is the slowness vector) in the coordinate system associated with the symmetry planes (i.e.,  $[x_1, x_3]$  is a vertical symmetry plane),  $V_{P0}$  is the vertical  $P$ -wave velocity [equation (1)], and  $\epsilon^{(i)}$  and  $\delta^{(i)}$  are Tsvankin's anisotropic parameters [equations (3), (4), (6), (7), (9)]. Equation (19) is fully linearized in the dimensionless anisotropic coefficients that are supposed to be small in the limit of weak anisotropy.

Equation (19) can be used to obtain the vertical slowness  $q \equiv p_3$  as an explicit function of the horizontal slowness components. This linearized solution has the form

$$q^2 = \left[ \frac{1}{V_{P0}^2} - p_1^2 - p_2^2 \right] - 2V_{P0}^2 \left\{ (p_1^2 + p_2^2) [p_1^2 (\epsilon^{(2)} - \delta^{(2)}) + p_2^2 (\epsilon^{(1)} - \delta^{(1)})] + \frac{p_1^2 \delta^{(2)} + p_2^2 \delta^{(1)}}{V_{P0}^2} + p_1^2 p_2^2 [\epsilon^{(1)} - \epsilon^{(2)} - \delta^{(3)}] \right\}. \quad (20)$$

As follows from equations (19) and (20), in the weak anisotropy approximation both the  $P$ -wave phase velocity  $V$  and the vertical component of the slowness vector  $q$  depend on only six quantities: the vertical velocity  $V_{P0}$  and five anisotropic parameters  $\epsilon^{(1)}$ ,  $\epsilon^{(2)}$ ,  $\delta^{(1)}$ ,  $\delta^{(2)}$ , and  $\delta^{(3)}$ . Since phase velocity determines all other kinematic signatures of a given mode, these six parameters fully control  $P$ -wave velocities and traveltimes in weakly orthorhombic media. Tsvankin (1996b) proved that this conclusion remains valid even for strong velocity anisotropy when the weak-anisotropy equations become numerically inaccurate.

It is also important to recognize that equation (20) contains the combinations  $\epsilon^{(2)} - \delta^{(2)}$  and  $\epsilon^{(1)} - \delta^{(1)}$ , which represent the linearized versions of the “anellipticity” coefficients  $\eta^{(2)}$  and  $\eta^{(1)}$  introduced in Tsvankin (1996b) by analogy with the Alkhalifah-Tsvankin coefficient  $\eta$ :

- $\eta^{(2)}$  – the VTI parameter  $\eta$  in the vertical symmetry plane  $[x_1, x_3]$ :

$$\eta^{(2)} = \frac{\epsilon^{(2)} - \delta^{(2)}}{1 + 2\delta^{(2)}}. \quad (21)$$

- $\eta^{(1)}$  – the VTI parameter  $\eta$  in the vertical symmetry plane  $[x_2, x_3]$ :

$$\eta^{(1)} = \frac{\epsilon^{(1)} - \delta^{(1)}}{1 + 2\delta^{(1)}}. \quad (22)$$

In the linearized weak-anisotropy approximation,  $\eta^{(2)} \approx \epsilon^{(2)} - \delta^{(2)}$  and  $\eta^{(1)} \approx \epsilon^{(1)} - \delta^{(1)}$ .

The kinematic equivalence between the symmetry planes of orthorhombic and VTI media implies that  $\eta^{(2)}$  and  $\eta^{(1)}$  are responsible for the “2-D”  $P$ -wave NMO-velocity function in the  $[x_1, x_3]$  and  $[x_2, x_3]$  planes, respectively. This equivalence, however, is valid only if the symmetry plane coincides with the dip plane of the reflector; otherwise, reflected rays propagate outside the vertical incidence plane and are influenced by azimuthal velocity variations.

Equation (20) contains another linear combination of the anisotropic coefficients ( $\epsilon^{(1)} - \epsilon^{(2)} - \delta^{(3)}$ ) that involves the parameter  $\delta^{(3)}$  specified for the horizontal symmetry plane  $[x_1, x_2]$  [equation (9)]. To identify this combination as another linearized  $\eta$  coefficient, this time corresponding to the  $[x_1, x_2]$  plane, let us recall the definition of  $\eta$  for VTI media (Alkhalifah and Tsvankin, 1995):

$$\eta \equiv \frac{1}{2} \left[ \frac{V_{\text{hor}}^2}{V_{\text{nmo}}^2(0)} - 1 \right]. \quad (23)$$

In applying equation (23) to the  $[x_1, x_2]$  symmetry plane, we have to keep in mind that  $x_1$  plays the role of the symmetry axis of the equivalent VTI medium [see equation (9)]. Hence, the “horizontal” velocity should be evaluated in the  $x_2$  direction ( $V_{\text{hor}} = V_{P0} \sqrt{1 + 2\epsilon^{(1)}}$ ), while the corresponding “ $V_{\text{nmo}}(0)$ ” is given by

$$V_{\text{nmo}}(0) = V_{P0} \sqrt{1 + 2\epsilon^{(2)}} \sqrt{1 + 2\delta^{(3)}}.$$

Substituting these values of  $V_{\text{hor}}$  and  $V_{\text{nmo}}(0)$  into equation (23), we define the  $\eta$  coefficient in the  $[x_1, x_2]$  plane as

$$\eta^{(3)} = \frac{\epsilon^{(1)} - \epsilon^{(2)} - \delta^{(3)}(1 + 2\epsilon^{(2)})}{(1 + 2\epsilon^{(2)})(1 + 2\delta^{(3)})}. \quad (24)$$

Evidently, for weak orthorhombic anisotropy  $\eta^{(3)}$  reduces to the linear combination ( $\epsilon^{(1)} - \epsilon^{(2)} - \delta^{(3)}$ ). The expression for  $\eta^{(3)}$  is more complicated than those for  $\eta^{(1)}$  and  $\eta^{(2)}$  because neither the velocity along the  $x_1$ -axis (the symmetry axis of the effective VTI medium) nor the coefficient  $\epsilon$  in the  $[x_1, x_2]$  plane are included in Tsvankin's parameterization (both would be redundant).

Introducing the values of  $\eta^{(1)}$ ,  $\eta^{(2)}$ , and  $\eta^{(3)}$  into the expression for the vertical slowness  $q$  [equation (20)], substituting  $q$  and its derivatives into the NMO equation (18) and carrying out further linearization in the anisotropic coefficients, we find the following weak-anisotropy approximation for  $P$ -wave NMO velocity (see Appendix A):

$$V_{\text{nmo}}^{-2}(\alpha, p_1, p_2) = \cos^2 \alpha \left\{ [V_{\text{nmo}}^{(2)}]^{-2} - p_1^2 + \sum_{i=1}^3 d_{1i} \eta^{(i)} \right\}$$

$$\begin{aligned}
 & + 2 \sin \alpha \cos \alpha \left\{ -p_1 p_2 + \sum_{i=1}^3 d_{2i} \eta^{(i)} \right\} \\
 & + \sin^2 \alpha \left\{ [V_{\text{nmo}}^{(1)}]^{-2} - p_2^2 + \sum_{i=1}^3 d_{3i} \eta^{(i)} \right\},
 \end{aligned} \tag{25}$$

where  $V_{\text{nmo}}^{(1,2)}$  [equations (A12)] are the linearized symmetry-plane NMO velocities from a horizontal reflector (i.e., the semi-axes of the corresponding NMO ellipse),  $\eta^{(i)}$  are the linearized versions of the parameters defined in equations (21), (22), and (24), and the quantities  $d_{ki}(p_1, p_2)$  are given in Appendix A. The azimuth  $\alpha$  in equation (25) is measured from the  $[x_1, x_3]$  symmetry plane. Note that for a horizontal reflector  $p_1 = p_2 = d_{ki} = 0$ , and equation (25) reduces to the NMO ellipse for a horizontal orthorhombic layer given by equation (14).

Although, as discussed above,  $P$ -wave phase velocity depends on six medium parameters, only *five* combinations of them ( $V_{\text{nmo}}^{(1)}$ ,  $V_{\text{nmo}}^{(2)}$ ,  $\eta^{(1)}$ ,  $\eta^{(2)}$ , and  $\eta^{(3)}$ ) determine the  $P$ -wave NMO velocity (25) in the weak anisotropy limit. This indicates that the NMO ellipse (25) for a dipping reflector ( $p_1 \neq 0$  and/or  $p_2 \neq 0$ ) can be inverted for the three  $\eta$  coefficients provided  $V_{\text{nmo}}^{(1)}$ ,  $V_{\text{nmo}}^{(2)}$ , and the orientation of the vertical symmetry planes have already been found using horizontal events.

To gain analytic insight into the possibility of recovering all three  $\eta$  coefficients from a single dipping event, let us consider a special case of the reflector strike aligned with one of the vertical symmetry planes. Suppose, for instance, that the dip plane of the reflector coincides with the  $[x_1, x_3]$  symmetry plane. Then the zero-offset ray is confined to the  $[x_1, x_3]$  plane, and the horizontal slowness component  $p_2$  is equal to zero. Evaluating the coefficients  $d_{ki}$  [equations (A2) – (A10)] for  $p_2 = 0$  and substituting the results into the NMO equation (25), we obtain

$$\begin{aligned}
 & V_{\text{nmo}}^{-2}(\alpha, p_1, p_2 = 0) = \\
 & = \cos^2 \alpha \left\{ [V_{\text{nmo}}^{(2)}]^{-2} - p_1^2 - 2p_1^2 \eta^{(2)} (4p_1^4 \tilde{V}^4 - 9p_1^2 \tilde{V}^2 + 6) \right\} \\
 & + \sin^2 \alpha \left\{ [V_{\text{nmo}}^{(1)}]^{-2} - 2p_1^2 [\eta^{(1)} - \eta^{(3)} + \eta^{(2)} (1 - p_1^2 \tilde{V}^2)] \right\},
 \end{aligned} \tag{26}$$

where  $\tilde{V} = \frac{1}{2} (V_{\text{nmo}}^{(1)} + V_{\text{nmo}}^{(2)})$ ; as discussed in Appendix A, in the linearized weak-anisotropy approximation it is possible to add any anisotropic terms to  $\tilde{V}$  without changing the final expression. Equation (26) shows that the semi-axes of the NMO ellipse are parallel to the dip and strike directions of the reflector. This result (which is valid for any strength of the anisotropy, see Grechka and Tsvankin, 1996, and Grechka et al., 1997) could be expected because the dip plane became a plane of symmetry for the whole model. If the azimuths of the sym-

metry planes have already been found from horizontal events, the orientation of the ellipse does not carry new information about the medium. Therefore, in this case the NMO ellipse for a single dipping event can be used to recover only *two* combinations of the medium parameters contained in the elliptical semi-axes. According to equation (26), the normal-moveout velocity in the dip plane of the reflector ( $\alpha = 0$ ) is given by

$$\begin{aligned}
 V_{\text{nmo}}(0, p_1) = & [V_{\text{nmo}}^{(2)}]^{-2} - p_1^2 \\
 & - 2p_1^2 \eta^{(2)} (4p_1^4 \tilde{V}^4 - 9p_1^2 \tilde{V}^2 + 6),
 \end{aligned} \tag{27}$$

which reduces to the weak-anisotropy approximation for the dip component of the  $P$ -wave NMO velocity in VTI media derived by Alkhalifah and Tsvankin (1995) [their equation (A-10)], if we choose  $\tilde{V}$  as  $V_{\text{nmo}}^{(2)}$  and recall that  $\eta^{(2)}$  and  $V_{\text{nmo}}^{(2)}$  are equivalent to the VTI parameters  $\eta$  and  $V_{\text{nmo}}(0)$ . Since the reflected rays on the dip line cannot deviate from the incidence (symmetry) plane,  $V_{\text{nmo}}(0, p_1)$  should indeed be given by the VTI equation due to the kinematic analogy between the symmetry planes of orthorhombic and VTI media (Tsvankin, 1996b). Conclusions of Alkhalifah and Tsvankin drawn for VTI media imply that the NMO velocity in the  $[x_1, x_3]$  plane can be inverted in a stable fashion for the coefficient  $\eta^{(2)}$ , if the reflector dip (represented by the horizontal slowness  $p_1$ ) reaches at least 20-25°.

Additional information about the medium parameters is contained in the NMO velocity  $V_{\text{nmo}}(\pi/2, p_1)$  measured in the strike direction (the second semi-axis of the NMO ellipse). Equation (26) indicates that the strike-line NMO velocity depends on the *difference*  $\eta^{(1)} - \eta^{(3)}$  rather than on the individual values of  $\eta^{(1)}$  and  $\eta^{(3)}$ . Therefore, if the  $[x_1, x_3]$  plane is orthogonal to the strike of a dipping reflector, the semi-axes of the NMO ellipse can be inverted for the parameter  $\eta^{(2)}$  and the difference  $\eta^{(1)} - \eta^{(3)}$  (the NMO velocities from a horizontal reflector are assumed to be known). Likewise, if the reflector strike is normal to the  $[x_2, x_3]$  plane, we can expect to obtain  $\eta^{(1)}$  and the difference  $\eta^{(2)} - \eta^{(3)}$ . (Note that in the weak-anisotropy approximation the definition of  $\eta^{(3)}$  is symmetric in the sense that it does not change if we use  $x_2$  as the symmetry axis of the effective VTI medium in the  $[x_1, x_2]$  plane.) Therefore, resolving all three  $\eta$  coefficients individually requires the presence of a dipping reflector with the strike sufficiently deviating from both vertical symmetry planes.

#### *P-wave NMO velocity for strong anisotropy*

The main purpose of applying the weak-anisotropy approximation to the NMO equation was to gain insight

into the dependence of the moveout function on the anisotropy parameters. In the actual inversion procedure described below, we use the *exact* equation (18) valid for any strength of the anisotropy. Therefore, it is necessary to find out whether the parameters  $V_{\text{nmo}}^{(1)}$ ,  $V_{\text{nmo}}^{(2)}$ ,  $\eta^{(1)}$ ,  $\eta^{(2)}$ , and  $\eta^{(3)}$  control the  $P$ -wave NMO velocity for models with strong velocity variations. It should be emphasized that here and below we use the *exact* definitions of the  $\eta$  coefficients [equations (21), (22) (24)] rather than their linearized weak-anisotropy approximations.

Note that if the dip plane of the reflector coincides with one of the vertical symmetry planes, the dip-line normal-moveout velocity is given by the VTI equations and, therefore, is fully determined by the zero-dip NMO velocity (i.e., the velocity from a horizontal reflector) and the corresponding  $\eta$  coefficient. For instance, if the  $[x_1, x_3]$  plane represents the dip plane of the reflector, the NMO velocity on the CMP line in the  $x_1$  direction depends just on the zero-dip value  $V_{\text{nmo}}^{(2)}$  and parameter  $\eta^{(2)}$  (Tsvankin, 1996b). Even in this special case, however, the strike-line NMO velocity is influenced by azimuthal velocity variations and has to be studied separately.

To show that the five parameters listed above are indeed sufficient to describe the 3-D  $P$ -wave NMO velocity for strongly anisotropic media, we performed several numerical tests. A typical result for a reflector with the dip azimuth diverging by  $30^\circ$  from the  $[x_1, x_3]$  symmetry plane is displayed in Figure 2. The NMO ellipse, explicitly defined in equation (12), was characterized by its semi-axes  $v_{e\ell 1}$  and  $v_{e\ell 2}$  (Figures 2a and 2b) and the rotation angle  $\beta$  between the larger semi-axis and the  $[x_1, x_3]$  symmetry plane (Figure 2c). All three parameters were calculated for a wide range of reflector dips as a function of the horizontal slowness  $p = \sqrt{p_1^2 + p_2^2}$ . In the first test, we varied the  $\epsilon$  and  $\delta$  coefficients keeping the parameters  $V_{\text{nmo}}^{(1)}$ ,  $V_{\text{nmo}}^{(2)}$ ,  $\eta^{(1)}$ ,  $\eta^{(2)}$ , and  $\eta^{(3)}$  constant (compare the solid and dashed lines). Clearly, the NMO ellipses for significantly different strongly anisotropic models that have the same parameters  $V_{\text{nmo}}^{(1,2)}$  and  $\eta^{(1,2,3)}$  practically coincide for all dips. In contrast, variation in the relevant parameter combinations  $\eta^{(1)}$  and  $\eta^{(2)}$  (dotted) leads to noticeable changes in the semi-axes and orientation of the NMO ellipse with increasing dip. The magnitude of the influence of  $\eta^{(1,2)}$  on normal moveout indicates that these coefficients can be obtained in a stable fashion from the NMO ellipse for a dipping event (provided the dip is not too mild).

Similar results have been obtained for a wide range of reflector azimuths and the values of anisotropic parameters. Thus, for a fixed orientation of the vertical symmetry planes, the exact NMO velocity  $V_{\text{nmo}}(\alpha, p_1, p_2)$  is

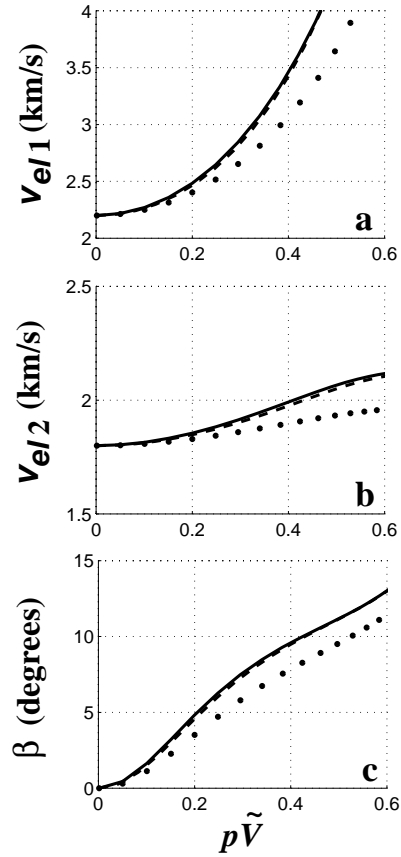


**Figure 2.** The dependence of the NMO ellipse from a dipping reflector on the parameters of an orthorhombic layer. The dip plane of the reflector makes an angle of  $30^\circ$  with the  $[x_1, x_3]$  symmetry plane; the reflector dip changes in accordance with the horizontal slowness (ray parameter)  $p = \sqrt{p_1^2 + p_2^2}$ . (a) and (b)  $P$ -wave NMO velocities in the directions of the semi-axes of the NMO ellipse; (c) the rotation angle  $\beta$  of the larger semi-axis with respect to the  $[x_1, x_3]$  symmetry plane. Solid line:  $V_{\text{nmo}}^{(1)} = 1.8$  km/s,  $V_{\text{nmo}}^{(2)} = 2.2$  km/s,  $\eta^{(1)} = 0.2$ ,  $\eta^{(2)} = 0.3$ ,  $\eta^{(3)} = 0.15$ ,  $\epsilon^{(1)} = 0.2$ ,  $\epsilon^{(2)} = 0.695$ ,  $\delta^{(1)} = 0$ ,  $\delta^{(2)} = 0.25$ ,  $\delta^{(3)} = -0.27$ . Dashed line: all  $V_{\text{nmo}}^{(i)}$  and  $\eta^{(i)}$  are the same as above, but  $\epsilon^{(1)} = -0.031$ ,  $\epsilon^{(2)} = 0.3$ ,  $\delta^{(1)} = -0.165$ ,  $\delta^{(2)} = 0$ ,  $\delta^{(3)} = -0.27$ . Dotted line:  $V_{\text{nmo}}^{(1)} = 1.8$  km/s,  $V_{\text{nmo}}^{(2)} = 2.2$  km/s,  $\eta^{(1)} = 0.1$ ,  $\eta^{(2)} = 0.2$ ,  $\eta^{(3)} = 0.15$ .  $\tilde{V}$  is defined by equation (A11).

a function of only five medium parameters –  $V_{\text{nmo}}^{(1,2)}$  and  $\eta^{(1,2,3)}$ . To recover these five parameters along with the symmetry-plane azimuths, we need a minimum of *six* moveout measurements which, in principle, can be obtained from at least two NMO ellipses corresponding to two distinct reflector dips and/or azimuths. In terms of the acquisition design, we need three or more CMP lines in different azimuthal directions to reconstruct the elliptical NMO-velocity dependencies and determine the hori-



zonal slowness components of the corresponding reflection events.

### Inversion of $P$ -wave NMO Velocity in a Single Layer

Although in principle the inverse problem can be posed for two arbitrary reflector dips, for the sake of simplicity we assume that one of the reflectors is horizontal. The NMO ellipse for the horizontal event [equation (14)] provides the azimuths of the symmetry planes and the NMO velocities  $V_{\text{nmo}}^{(1,2)}$  within them. The azimuthally dependent zero-offset traveltimes of the dipping reflection can be used to find the horizontal slowness components  $p_1$  and  $p_2$  of the zero-offset ray, while the corresponding NMO ellipse can be inverted for the parameters  $\eta^{(1,2,3)}$ . We formulate the conditions necessary for resolving all three  $\eta$  coefficients and study the stability of the inversion procedure to errors in the input data.

This algorithm relies on the difference between the symmetry-plane NMO velocities from a horizontal reflector to find the orientation of the symmetry planes. It may happen, however, that  $V_{\text{nmo}}^{(1)} = V_{\text{nmo}}^{(2)}$  ( $\delta^{(1)} = \delta^{(2)}$ ), and the NMO ellipse for horizontal events degenerates into a circle. In this case (not discussed here), we need *two* different dipping events to recover the symmetry-plane azimuths and three  $\eta$  coefficients.

If  $V_{\text{nmo}}^{(1,2)}$  and the orientation of the symmetry planes have been obtained, the elements of the matrix  $\mathbf{W}$  for a dipping event with the horizontal slowness components  $p_1$  and  $p_2$  become functions of  $\eta^{(1,2,3)}$  [see equation (16)]:

$$W_{ij}(\eta^{(1)}, \eta^{(2)}, \eta^{(3)}) = q_{ij} (2\delta_{ij} - 1) \frac{p_1 q_1 + p_2 q_2 - q}{q_{11} q_{22} - q_{12}^2}, \quad (28)$$

$$(i, j = 1, 2),$$

$\delta_{ij}$  is the Kronecker's  $\delta$ . Therefore, the three  $\eta$  coefficients can be found numerically by solving the following least-squares problem:

$$\mathcal{F}_P \equiv \sum_{i,j=1}^2 [\hat{W}_{ij} - W_{ij}(\eta^{(1)}, \eta^{(2)}, \eta^{(3)})]^2 = \min, \quad (29)$$

where  $\hat{\mathbf{W}}$  is the matrix that determines the NMO ellipse reconstructed from azimuthally dependent moveout data. Since the symmetric matrix  $\mathbf{W}$  has three independent components, the system (29) contains three nonlinear equations with three unknowns. Numerical tests performed with various initial guesses for an error-free matrix  $\hat{\mathbf{W}}$  showed that the inversion algorithm (we used the simplex method) successfully converges towards the correct values of  $\eta^{(1,2,3)}$  (or their correct combinations, if the parameters cannot be resolved individually).

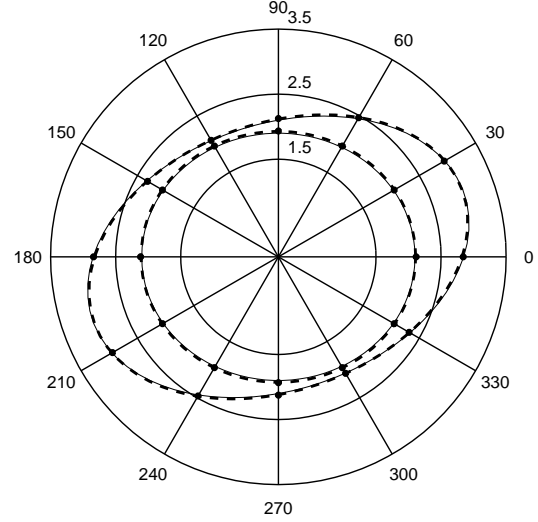


**Figure 3.** Comparison of the  $P$ -wave NMO ellipses for horizontal and dipping events from equations (14) and (18) (solid lines) with the moveout (stacking) velocity (dots) obtained by least-squares fitting of a hyperbola to the exact traveltimes computed for spreadlength equal to the distance between the CMP and the reflector. The dashed lines mark the best-fit ellipses approximating the measured moveout velocity (i.e., traced through the dots). The dip plane of the reflector deviates by  $30^\circ$  from the  $[x_1, x_3]$  symmetry plane (azimuth  $0^\circ$  on the plot) of the layer; reflector dip is equal to  $40^\circ$ . The layer parameters are  $V_{\text{nmo}}^{(1)} = 1.90$  km/s,  $V_{\text{nmo}}^{(2)} = 2.10$  km/s,  $\eta^{(1)} = 0.1$ ,  $\eta^{(2)} = 0.05$ ,  $\eta^{(3)} = 0.15$  ( $\epsilon^{(1)} = 0.1$ ,  $\epsilon^{(2)} = 0.17$ ,  $\delta^{(1)} = 0$ ,  $\delta^{(2)} = 0.11$ ,  $\delta^{(3)} = -0.16$ ).

The first step in this inversion procedure is determination of the parameters of NMO ellipses from finite-spread moveout data that may be influenced by non-hyperbolic moveout. However, as shown by Grechka and Tsvankin (1996) and Grechka et al. (1997), conventional-spread  $P$ -wave moveout in an orthorhombic layer is typically close to hyperbolic with the moveout (stacking) velocity well-approximated by the analytic NMO value from equation (18). Numerical test in Figure 3, performed on the spreadlength equal to the CMP-reflector distance, confirms this conclusion for both the horizontal and dipping reflector. The inversion of the two ellipses reconstructed from finite-spread moveout data yields accurate estimates of the  $\eta$  coefficients:  $\eta^{(1)} = 0.084$  (instead of 0.1),  $\eta^{(2)} = 0.041$  (instead of 0.05), and  $\eta^{(3)} = 0.123$  (instead of 0.15). The higher error in the parameter  $\eta^{(3)}$  is due to the fact that this coefficient mostly influences near-horizontal velocity variations (see the discussion below).

The results for the model in Figure 3, as well as those for a number of other models we have studied, show that a certain *percentage* error in the NMO velocity translates into a similar *absolute* error in the coefficients  $\eta^{(1)}$  and

$\eta^{(2)}$ ; the same conclusion was drawn previously for  $\eta$  inversion in VTI media by Alkhalifah and Tsvankin (1995) and Grechka and Tsvankin (1996). In the example from Figure 3, the maximum error in the NMO velocity for both horizontal and dipping events is smaller than 1.5%. The magnitude of nonhyperbolic moveout for horizontal reflectors increases with  $\eta^{(1)}$  and  $\eta^{(2)}$ , but the associated NMO-velocity error on conventional spreads seldom exceeds 2.5-3%. If the data after hyperbolic moveout correction show residual moveout, it is possible to obtain a more accurate estimate of  $V_{\text{nmo}}$  by applying a nonhyperbolic moveout equation (Grechka and Tsvankin, 1997).

The only source of errors in the example from Figure 3 is the influence of nonhyperbolic moveout, which proved to be relatively small. A more general analysis of the influence of errors in the input data is presented in Figure 4. If the components of the matrices  $W$  are taken from the two exact NMO ellipses, the inversion of equation (28) gives almost perfect results with the recovered  $\eta^{(1,2,3)}$  different by no more than 0.005 from the actual values. These minor errors are explained by the fact that in the inversion procedure we intentionally used inaccurate values of  $V_{P0} = \tilde{V} = 2.0$  km/s [see equation (A11)] (the actual  $V_{P0} = 1.9$  km/s) and  $V_{S0} = V_{P0}/2 = 0.95$  km/s (the actual  $V_{S0} = 0.6$  km/s). This is another illustration of the negligible influence of the vertical velocities (which are generally unknown) on the NMO function; clearly, it is justified to use reasonable estimates for  $V_{P0}$  and  $V_{S0}$  in the inversion procedure.

It is clear from Figure 4 that different  $\eta$  coefficients are most sensitive to errors in different measured quantities. For instance,  $\eta^{(2)}$  (the solid line in Figures 4a and 4b) strongly depends on the *larger* semi-axes of both NMO ellipses (which are close to the  $[x_1, x_3]$  plane) and is almost insensitive to the changes in the smaller semi-axes (Figures 4c and 4d). These conclusions are in good agreement with the analytic results obtained in the weak-anisotropy approximation. As indicated by equation (26),  $\eta^{(2)}$  is the only anisotropic coefficient that controls the larger semi-axis of the NMO ellipse (i.e., the dip-line NMO velocity) for a reflector with the dip plane parallel to the  $x_1$  axis. The inversion of the dip-line NMO velocity for  $\eta^{(2)}$  in this case involves just  $V_{\text{nmo}}^{(2)}$  – the zero-dip NMO velocity in the same ( $x_1$ ) direction [see equation (27)]. Since for the model in Figure 4 the azimuth of the dip plane is closer to the  $x_1$  than to the  $x_2$  axis,  $\eta^{(2)}$  remains primarily responsible for the larger semi-axis of the ellipse for the dipping event and is highly sensitive to the zero-dip NMO velocity in the  $x_1$  direction ( $V_{\text{nmo}}^{(2)}$ ).

Equation (26) also shows that if  $[x_1, x_3]$  represents the dip plane of the reflector,  $\eta^{(1)}$  and  $\eta^{(3)}$  influence just the strike-line NMO velocity (i.e., the smaller semi-axis of

the NMO ellipse), and only as the *difference*  $\eta^{(1)} - \eta^{(3)}$ . In addition, note that the NMO velocity in the strike direction depends on  $V_{\text{nmo}}^{(1)}$  but does not contain  $V_{\text{nmo}}^{(2)}$  [equation (26)]. This allows us to understand the results of the inversion for  $\eta^{(1)}$  and  $\eta^{(3)}$  in Figures 4a,b,c,d. First, both  $\eta^{(1)}$  and  $\eta^{(3)}$  are sensitive mostly to the errors in the smaller semi-axis of the NMO ellipse for the dipping event, as well as in  $V_{\text{nmo}}^{(1)}$ . Second, we were able to restore the difference  $\eta^{(1)} - \eta^{(3)}$  with a much higher accuracy than either of the coefficients individually (see Figure 4c,d).

The influence of the errors in the orientation of the ellipses (Figures 4e and 4f) is more difficult to interpret, but it can also be explained in terms of the general weak-anisotropy approximation (26). The values of  $\eta^{(1)}$  and  $\eta^{(2)}$  are reasonably stable with respect to estimates of the rotation angles  $\beta$ , while the coefficient  $\eta^{(3)}$  is sensitive to errors in the orientation of the ellipse for the dipping event.

Overall, if the dip plane of the reflector is closer to the  $x_1$  direction, the coefficient most tightly constrained by  $P$ -wave moveout data is  $\eta^{(2)}$ . This is not surprising since the parameter  $\eta^{(2)}$  is fully responsible for the dip-dependent NMO velocity in the  $[x_1, x_3]$  plane. In contrast, the coefficient  $\eta^{(3)}$  proved to be most sensitive to errors in the input data, especially in the orientation and the smaller semi-axis of the NMO ellipse for the dipping event. Since  $\eta^{(3)}$  is defined in the horizontal symmetry plane, its influence on NMO velocity for moderate reflector dips (e.g., a dip of  $40^\circ$  in Figure 4) is smaller than that of  $\eta^{(1)}$  and  $\eta^{(2)}$ . A more stable estimate of  $\eta^{(3)}$  requires the presence of a steeper reflector with the dip plane sufficiently deviating from the vertical symmetry planes.

In summary, the inversion of the  $P$ -wave NMO ellipses corresponding to reflections from a horizontal and dipping interface in a homogeneous orthorhombic layer may yield the orientation of the vertical symmetry planes, two symmetry-plane NMO velocities from a horizontal reflector [equation (15)], and three anisotropic parameters  $\eta^{(1,2,3)}$  specified by equations (21) – (24). Since the  $\eta$  coefficients control the dip-dependence of NMO velocity and make no contribution to moveout for horizontal events, the dipping interface used in the inversion should not be too close to horizontal. In agreement with the results of Alkhalifah and Tsvankin (1995) for  $\eta$  inversion in VTI media, the estimates of the anisotropic parameters become unstable for mild dips below  $20$ - $25^\circ$ .

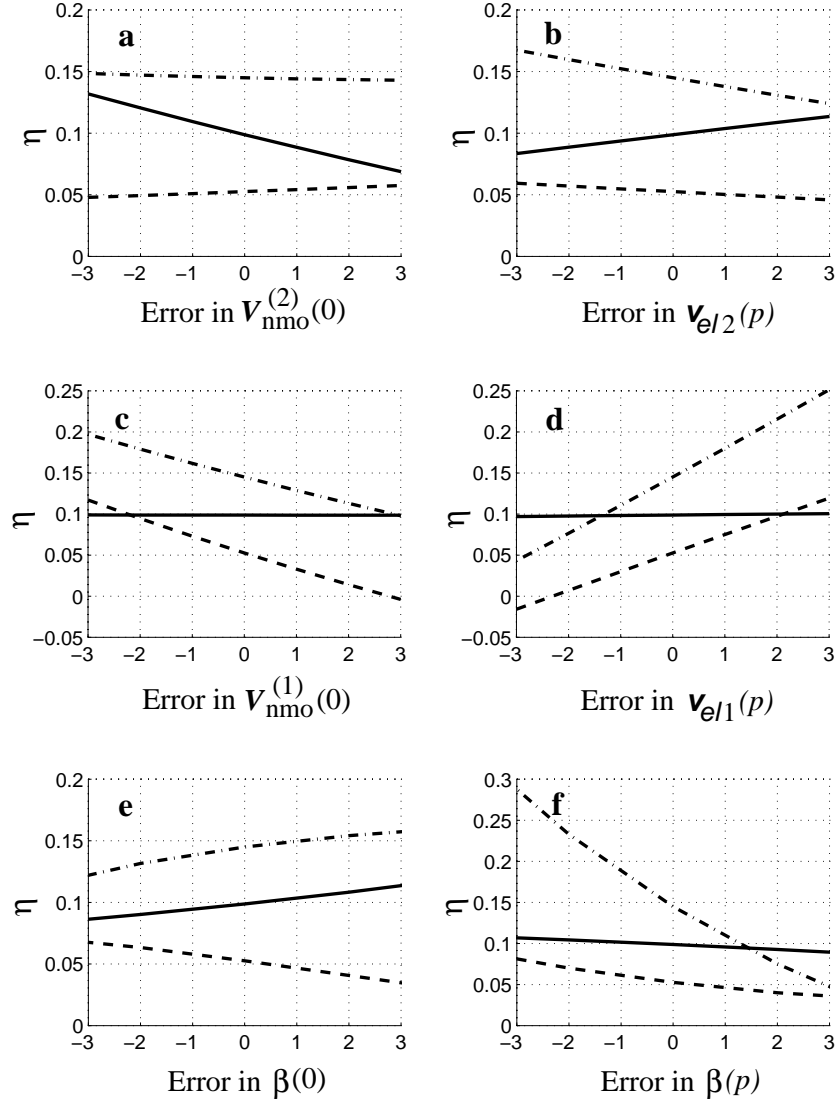


**Figure 4.** Inversion of the  $P$ -wave NMO ellipses from a horizontal and dipping reflector for  $\eta^{(1)}$  (dashed line),  $\eta^{(2)}$  (solid line), and  $\eta^{(3)}$  (dash-dotted line). The dip plane makes an angle of  $30^\circ$  with the  $[x_1, x_3]$  symmetry plane, the dip is  $40^\circ$ . (a) and (c) – errors in the semi-axes of the ellipse for the horizontal event (in %); (b) and (d) – errors in the semi-axes of the ellipse for dipping event (in %); (e) – errors in the orientation angle  $\beta(0)$  of the NMO ellipse for the horizontal event (in degrees); (f) – errors in the orientation angle  $\beta(p)$  of the NMO ellipse for the dipping event (in degrees). The actual parameters are  $\eta^{(1)} = 0.05$ ,  $\eta^{(2)} = 0.10$ , and  $\eta^{(3)} = 0.15$ . The inversion results in the absence of errors:  $\eta^{(1)} = 0.053$ ,  $\eta^{(2)} = 0.099$ , and  $\eta^{(3)} = 0.145$ .

### Moveout Inversion for Vertically Inhomogeneous Media

#### Dix-type layer stripping in orthorhombic media

The inversion approach outlined above can be extended to horizontally layered orthorhombic media above a dipping reflector (Figure 5) using the generalized Dix-type equation developed by Grechka et al. (1997). As before, it is assumed that we have a minimum of three differently oriented CMP lines (Figure 5) that allow us to re-

construct the effective NMO ellipses [i.e., the matrices  $\mathbf{W}(L)$ ] for reflections from horizontal and dipping interfaces. Also, we use the zero-offset sections along the same lines to obtain the horizontal slowness components  $p_1$  and  $p_2$  of the zero-offset ray for the dipping event. As shown by Grechka et al. (1997), the matrix  $\mathbf{W}(L)$  that describes the effective NMO ellipse from a horizontal or dipping reflector can be found by the following averaging of the interval matrices  $\mathbf{W}_\ell$ :

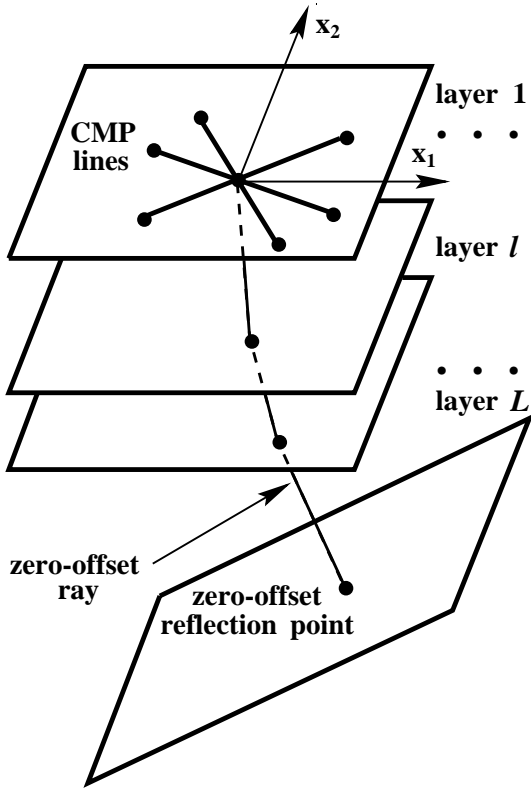


**Figure 5.** A horizontally layered orthorhombic medium above a dipping reflector.

$$\mathbf{W}^{-1}(L) = \frac{1}{\tau(L)} \sum_{\ell=1}^L \tau_{\ell} \mathbf{W}_{\ell}^{-1}, \quad (30)$$

where  $\tau_{\ell}$  are the interval zero-offset traveltimes and  $\tau(L) = \sum_{\ell=1}^L \tau_{\ell}$ . Equation (30) is valid for vertically inhomogeneous overburden (Figure 5) with arbitrary symmetry in each layer. It should be emphasized that all interval matrices in equation (30) are evaluated for the horizontal slownesses  $p_1$  and  $p_2$  of the zero-offset ray from the dipping reflector.

Given the effective matrices for reflections from the top and bottom of layer  $\ell$  and the corresponding zero-offset traveltimes, the interval matrix  $\mathbf{W}_{\ell}$  can be obtained by Dix-type differentiation,

$$\mathbf{W}_{\ell}^{-1} = \frac{\tau(\ell)\mathbf{W}^{-1}(\ell) - \tau(\ell-1)\mathbf{W}^{-1}(\ell-1)}{\tau(\ell) - \tau(\ell-1)}. \quad (31)$$

Evidently, instead of the squared NMO *velocities* in the conventional Dix equation, equations (30) and (31) contain the inverse of the *matrices*  $\mathbf{W}$  responsible for the interval NMO ellipses. Only if the model has a throughgoing symmetry plane (i.e., the dip plane coincides with a plane of symmetry in all layers), equation (30) splits into two rms-averaging equations for the NMO velocities in the dip and strike directions (Grechka

et al., 1997). Also, as shown by Grechka et al., the rms average of NMO velocities taken at a fixed azimuth provides a good approximation for equation (30) in this direction, if the interval NMO ellipses are close enough to circles. In general, however, application of the standard Dix differentiation of NMO velocity may lead to errors in the interval values. For instance, as shown in Appendix B, rms averaging of interval NMO velocities always underestimates the effective velocity near intersections of interval NMO ellipses.

In contrast to the conventional Dix equation, the only components of equation (30) that can be obtained from the data *directly* are the effective matrix  $\mathbf{W}(L)$  and the zero-offset traveltime  $\tau(L)$  for the reflection from the dipping interface. The interval matrices  $\mathbf{W}$  in the horizontal layers generally correspond to *non-existing* reflectors normal to the slowness vector of the zero-offset ray. To carry out the layer-stripping described by equation (31), we need to recalculate  $\mathbf{W}(\ell)$  and  $\tau(\ell)$  from the values of  $p_1$  and  $p_2$  for available reflection events to those of the dipping reflector; it is discussed in more detail below.

Here, we use the generalized Dix equation (30) to develop a layer-stripping procedure for an orthorhombic overburden. First, we carry out the Dix-type differentiation (31) of the NMO ellipses for reflections from horizontal interfaces to obtain the interval matrices  $\mathbf{W}_{\ell}$  for the horizontal events. Since the slowness vector of the zero-offset ray from all horizontal boundaries is vertical ( $p_1 = p_2 = 0$ ), the effective matrices for the top and bottom of each layer needed in equation (31) can be obtained from the data directly, without any recalculation from one ray-parameter value to another. The interval NMO ellipses for horizontal reflectors yield the orientation of the symmetry planes in each layer [described by the rotation angles  $\beta_{\ell}(0)$ ] and the symmetry-plane NMO velocities  $V_{\text{nmo},\ell}^{(1)}$  and  $V_{\text{nmo},\ell}^{(2)}$ . Note that we do not assume that the medium has throughgoing vertical symmetry planes (i.e.,  $\beta_{\ell}(0)$  is not necessarily constant); the generalized Dix equation allows the orientation of the symmetry planes to vary from layer to layer in an arbitrary fashion.

After performing the Dix-type differentiation for horizontal reflections, we can use dipping events to determine the interval values of  $\eta_{\ell}^{(1,2,3)}$ . The results of the single-layer inversion show that to resolve all three  $\eta$  coefficients in each interval, we need at least one dipping reflector with the dip plane sufficiently deviating from the symmetry planes of this layer. Realistically, we have to determine the effective values of the anisotropic coefficients between the velocity picks for the dipping events, whether the corresponding intervals are homogeneous or not.

The inversion procedure in the first (subsurface) layer [equations (28) and (29)], yields the values of

$V_{\text{nmo},1}^{(1)}$ ,  $V_{\text{nmo},1}^{(2)}$ ,  $\beta_1(0)$ ,  $\eta_1^{(1)}$ ,  $\eta_1^{(2)}$ , and  $\eta_1^{(3)}$  that can be used to calculate the interval matrix  $\mathbf{W}_1$  for the parameters  $p_1$  and  $p_2$  corresponding to the dipping reflector in the *second* layer. Then we determine the effective matrix  $\mathbf{W}(2)$  from the azimuthally dependent NMO velocity for this dipping reflector (along with the zero-offset traveltime) and apply equation (31) to obtain the interval matrix  $\mathbf{W}_2$  in the second layer. The matrix  $\mathbf{W}_2$  and the interval values  $V_{\text{nmo},2}^{(1)}$ ,  $V_{\text{nmo},2}^{(2)}$  found from the horizontal events are inverted for the parameters  $\eta_2^{(1)}$ ,  $\eta_2^{(2)}$ , and  $\eta_2^{(3)}$ . This layer-stripping procedure is continued downward, as long as both horizontal and dipping events are available. Note that to determine the interval matrix in any layer  $\mathbf{W}_L$ , the matrices  $\mathbf{W}_\ell$  in all overlying layers  $\ell = 1, \dots, L-1$  need to be recalculated to the values of  $p_1$  and  $p_2$  for the dipping reflector in layer  $L$ .

In addition to the effective matrices  $\mathbf{W}$  for the reflection from the top and bottom of a layer, equation (31) contains zero-offset traveltimes that also depend on the parameters  $p_1$  and  $p_2$ . Therefore, implementation of the Dix-type layer-stripping procedure described above requires computing not only the interval matrices  $\mathbf{W}_\ell$ , but also the interval traveltimes  $\tau_\ell$  as functions of  $p_1$  and  $p_2$ . Although  $P$ -wave traveltimes in general depend on the vertical velocity and five  $\epsilon$  and  $\delta$  coefficients, below we show that the moveout parameters  $V_{\text{nmo}}$ ,  $V_{\text{nmo}}^{(2)}$ ,  $\eta^{(1)}$ ,  $\eta^{(2)}$ , and  $\eta^{(3)}$  are sufficient for converting the vertical zero-offset traveltime  $\tau_{0,\ell}$  in a horizontal orthorhombic layer (known from horizontal events) into the traveltime along an arbitrary oblique ray. The one-way traveltime  $\tau(p)$  in the  $\ell$ -th layer (below we omit the index  $\ell$  for brevity) can be calculated as the ratio of the layer thickness  $z$  and the vertical component of the group velocity  $g_3$ ,

$$\tau(p) = \frac{z}{g_3} = \frac{\tau_0 V_{P0}}{g_3}, \quad (32)$$

where  $\tau_0$  is the vertical zero-offset traveltime and  $V_{P0}$  is the vertical velocity. For the vertical group-velocity component, Grechka et al. (1997) obtained the following equation:

$$g_3 = \frac{1}{q - p_1 q_{,1} - p_2 q_{,2}}, \quad (33)$$

where  $q_{,i}$  are the partial derivatives of the vertical component of slowness  $q \equiv p_3$  with respect to the horizontal components  $p_i$ . Substituting equation (33) into equation (32) yields

$$\tau(p) = \tau_0 V_{P0} (q - p_1 q_{,1} - p_2 q_{,2}). \quad (34)$$

Numerical analysis of equation (34) indicates that the ratio  $\tau(p)/\tau_0$  expressed through the parameters  $p_1$  and  $p_2$  is indeed fully controlled by the two NMO velocities and three  $\eta$  coefficients responsible for the NMO-velocity function (Figure 6).

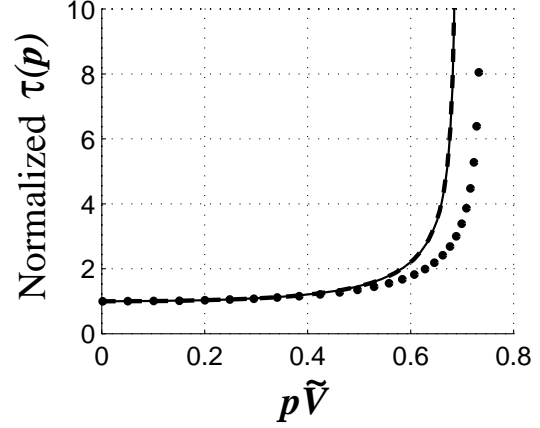


**Figure 6.** Dependence of the traveltime  $\tau(p)$  along an oblique ray on the parameters of a (horizontal) orthorhombic layer. Solid line:  $V_{\text{nmo}}^{(1)} = 1.8$  km/s,  $V_{\text{nmo}}^{(2)} = 2.2$  km/s,  $\eta^{(1)} = 0.2$ ,  $\eta^{(2)} = 0.3$ ,  $\eta^{(3)} = 0.15$ ,  $\epsilon^{(1)} = 0.2$ ,  $\epsilon^{(2)} = 0.695$ ,  $\delta^{(1)} = 0$ ,  $\delta^{(2)} = 0.25$ ,  $\delta^{(3)} = -0.27$ . Dashed line: all  $V_{\text{nmo}}^{(i)}$  and  $\eta^{(i)}$  are the same as above,  $\epsilon^{(1)} = -0.031$ ,  $\epsilon^{(2)} = 0.3$ ,  $\delta^{(1)} = -0.165$ ,  $\delta^{(2)} = 0$ ,  $\delta^{(3)} = -0.27$ . Dotted line:  $V_{\text{nmo}}^{(1)} = 1.8$  km/s,  $V_{\text{nmo}}^{(2)} = 2.2$  km/s,  $\eta^{(1)} = 0.1$ ,  $\eta^{(2)} = 0.2$ ,  $\eta^{(3)} = 0.15$ .  $\tilde{V}$  is defined by equation (A11).

The principle of our layer-stripping procedure is close to that of the 2-D  $\eta$ -inversion algorithm in VTI media described by Alkhalifah and Tsvankin (1995). Here, however, we operate with NMO ellipses influenced by the 3-D character of wave propagation, rather than with normal-moveout velocities measured in a vertical symmetry plane of the model.

The stability of the interval parameter estimation is influenced by the errors in the single-layer inversion procedure discussed above, as well as by the magnification of errors caused by the Dix-type differentiation. As in the conventional Dix velocity analysis, the accuracy in the interval values is inversely proportional to the thickness of the interval. Let us denote the relative time thickness of the  $\ell$ -th layer (for which the differentiation is performed) as

$$\sigma_\ell = \frac{\tau_\ell}{\tau(\ell)}. \quad (35)$$

Equation (35) allows us to rewrite equation (31) in the form

$$\mathbf{W}_\ell^{-1} = \frac{1}{\sigma_\ell} [\mathbf{W}^{-1}(\ell) - (1 - \sigma_\ell) \mathbf{W}^{-1}(\ell - 1)] \quad (36)$$

which explicitly shows that, for small  $\sigma_\ell$ , any errors in effective NMO ellipses will propagate into the errors in interval ellipses with the magnification factor  $1/\sigma_\ell$ .

**Synthetic example**

To demonstrate the feasibility of our parameter-estimation algorithm, we applied it to the inversion of the exact (ray-traced) reflection traveltimes in a three-layer orthorhombic model with a throughgoing dipping reflector (Figure 7). NMO ellipses for horizontal and dipping events were obtained by hyperbolic semblance analysis on spreadlengths close to and even exceeding the CMP-reflector distance. In principle, these estimates may be distorted by the influence of nonhyperbolic moveout that is usually enhanced by vertical inhomogeneity. However, deviations of the exact traveltimes from the hyperbola parameterized by the analytic NMO velocity become pronounced only for offsets that exceed the distance between the CMP and the reflector (Figure 8). Note that the moveouts shown in Figure 8 are calculated for rays that crossed three orthorhombic layers with different orientation of the vertical symmetry planes and, therefore, bear the full impact of azimuthal anisotropy and vertical inhomogeneity. It is interesting that the magnitude of nonhyperbolic moveout is much more significant for the horizontal reflector, while the moveout of the dipping event stays close to the analytic hyperbola up to relatively large offsets. The same conclusion was drawn by Tsvankin (1995) in his study of dip-plane moveout for vertical transverse isotropy. Indeed, if both the spreadlength and the distance between the CMP and the reflector are fixed, the range of take-off angles for reflected rays decreases with dip, which mitigates the influence of anisotropy on the traveltimes and reduces nonhyperbolic moveout.

Although the errors in the effective NMO ellipses are slightly higher (mostly for horizontal events) than those in the single-layer model (Figure 3), the accuracy of our NMO equations is quite sufficient for a stable recovery of the anisotropic parameters (Table 1). Even in the relatively thin deepest layer, the maximum error in the  $\eta$  coefficients is close to just 0.02, while the overall maximum error is slightly over 0.03. The consistently negative errors in all anisotropic coefficients are explained by the fact that the increasing influence of nonhyperbolic moveout with depth leads to overestimation of the interval NMO velocities from horizontal reflectors. (This interval error, however, is not substantial because the distortion in the NMO velocities from both the top and bottom of each layer has the same sign.) Since the errors in the NMO velocities from dipping reflectors are almost negligible, the higher values of  $V_{\text{nmo}}^{(1,2)}$  have to be compensated by smaller coefficients  $\eta^{(1,2,3)}$  to match the NMO ellipses for the dipping events.

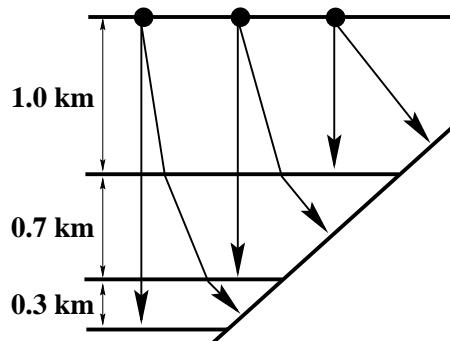


**Figure 7.** A 2-D sketch of the layered orthorhombic model used to test the inversion algorithm. The azimuth  $\beta(0)$  of the  $[x_1, x_3]$  symmetry plane changes with depth: Layer 1 -  $\beta_1(0) = 0^\circ$ , Layer 2 -  $\beta_2(0) = -10^\circ$ , Layer 3 -  $\beta_3(0) = -20^\circ$ ; the parameters of each layer are given in Table 1. The azimuth of the dip plane of the reflector is  $30^\circ$ , the dip is  $40^\circ$ .

**Discussion and Conclusions**

We have shown that the exact  $P$ -wave normal-moveout velocity in orthorhombic media is fully controlled by the orientation of the vertical symmetry planes and five medium parameters – two symmetry-plane NMO velocities from a horizontal reflector ( $V_{\text{nmo}}^{(1)}$  and  $V_{\text{nmo}}^{(2)}$ ) and three anisotropic coefficients ( $\eta^{(1)}$ ,  $\eta^{(2)}$ , and  $\eta^{(3)}$ ). The parameters  $\eta^{(1,2)}$  are introduced in the vertical symmetry planes by analogy with the Alkhalifah-Tsvankin “anelipticity” coefficient  $\eta$  for vertical transverse isotropy, and  $\eta^{(3)}$  is a similar parameter defined in the horizontal symmetry plane. The velocities  $V_{\text{nmo}}^{(1)}$  and  $V_{\text{nmo}}^{(2)}$  are responsible for normal moveout from horizontal reflectors, while  $\eta^{(1,2,3)}$  determine the dip dependence of NMO velocity. It should be emphasized that these five parameters govern the NMO function expressed through the horizontal slowness components of the zero-offset ray (rather than the dip and azimuth of the reflector normal) – quantities that can be obtained from reflection slopes on zero-offset sections.

Both the modeling and inversion parts of this paper are based on the fact that the azimuthal dependence of NMO velocity for any pure mode has an elliptical shape in the horizontal plane (Grechka and Tsvankin, 1996). A minimum of three azimuthal moveout measurements is required to reconstruct the NMO ellipse for a given reflection event. Then the three parameters that define the ellipse (e.g., its semi-axes and the orientation angle) can be inverted for the relevant combinations of the medium coefficients. Here, we develop this inversion procedure for a vertically inhomogeneous orthorhombic medium above a dipping reflector using the analytic expressions for the NMO ellipse given by Grechka and Tsvankin (1996) and Grechka et al. (1997).

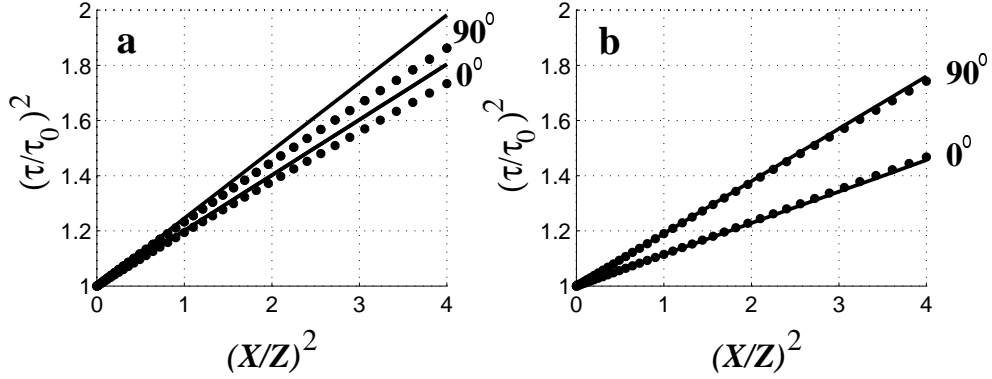


**Figure 8.** Accuracy of the hyperbolic moveout equation for the model from Figure 7. Dots show  $P$ -wave traveltimes computed by 3-D anisotropic ray tracing; solid lines are hyperbolic moveout curves parameterized by the NMO velocity calculated using the generalized Dix equation (30). (a) Reflection from the deepest horizontal boundary (bottom of Layer 3); (b) Reflection from the segment of the dipping interface in Layer 3.  $Z$  is the distance between the CMP and the reflector,  $X$  is the source-receiver offset.

Layer	Correct values					Inverted values				
	$V_{\text{nmo}}^{(1)}$ (km/s)	$V_{\text{nmo}}^{(2)}$ (km/s)	$\eta^{(1)}$	$\eta^{(2)}$	$\eta^{(3)}$	$V_{\text{nmo}}^{(1)}$ (km/s)	$V_{\text{nmo}}^{(2)}$ (km/s)	$\eta^{(1)}$	$\eta^{(2)}$	$\eta^{(3)}$
1	2.500	2.763	0.100	0.050	0.150	2.540	2.794	0.072	0.040	0.127
2	2.900	3.177	0.150	0.100	0.150	2.969	3.226	0.118	0.081	0.127
3	3.200	3.786	0.200	0.150	0.200	3.254	3.834	0.183	0.129	0.179

**Table 1.** Comparison of the inverted and actual values of the interval parameters for the model from Figure 2. The maximum source-receiver offsets used in estimating moveout velocity are as follows: horizontal and dipping reflectors in Layer 3 – 1.8 km (spreadlength-to-depth ratio  $X_{\text{max}}/Z = 0.9$ ); Layer 2 – 1.8 km ( $X_{\text{max}}/Z = 1.06$ ); Layer 1 – 1.2 km ( $X_{\text{max}}/Z = 1.2$ ).

First, we studied the inversion of reflection traveltimes from horizontal and dipping reflectors in a single orthorhombic layer. The NMO ellipse for horizontal events yields the orientation of the vertical symmetry planes and the velocities  $V_{\text{nmo}}^{(1)}$  and  $V_{\text{nmo}}^{(2)}$ . Then we use normal moveout of at least one dipping event along with the obtained values of  $V_{\text{nmo}}^{(1,2)}$  to find the coefficients  $\eta^{(1)}$ ,  $\eta^{(2)}$ , and  $\eta^{(3)}$ . Since  $\eta^{(1,2,3)}$  control the dip-dependence of NMO velocity and make no contribution to moveout for horizontal events, the dipping interface used in the inversion should not be too close to horizontal. The presence of a sufficient dip, however, does not guarantee the recovery of all three  $\eta$  parameters. If the dip-plane azimuth is close to the  $[x_1, x_3]$  symmetry plane, we can resolve only the coefficient  $\eta^{(2)}$  (defined in this plane) and the difference of the other two coefficients ( $\eta^{(1)} - \eta^{(3)}$ ). Likewise, if the the dip line is close to the  $[x_2, x_3]$  plane, the inversion yields the parameter  $\eta^{(1)}$  and the difference ( $\eta^{(2)} - \eta^{(3)}$ ). Estimation of the individual values of all three coefficients becomes reasonably stable if the reflector azimuth makes an angle of 20-25° or more with the nearest symmetry plane. For dips in the most common range of 30-50°, the

sensitivity to the errors in input data is higher for  $\eta^{(3)}$  than for the other two coefficients since this parameter is largely determined by near-horizontal velocity variations outside the vertical symmetry planes.

Extension of our inversion scheme to vertically inhomogeneous media is based on the generalized Dix equation (Grechka et al., 1997) that operates with the matrices responsible for interval NMO ellipses evaluated for the horizontal slowness components of the zero-offset ray. For horizontal events, our procedure is similar to the conventional Dix differentiation because the effective NMO ellipses corresponding to the reflections from the top and bottom of each *horizontal* layer can be obtained from the data directly. In the case of dipping events, however, it is necessary to carry out a full-scale layer-stripping procedure by recalculating the NMO ellipses and zero-offset traveltimes in the overburden to the ray-parameter values corresponding to the dipping reflector. As a result of the layer stripping, we obtain the orientation of symmetry planes and the five relevant parameters ( $V_{\text{nmo}}^{(1)}$  and  $V_{\text{nmo}}^{(2)}$ ) and three anisotropic coefficients ( $\eta^{(1)}$ ,  $\eta^{(2)}$ , and  $\eta^{(3)}$ ) in each layer. Our stripping algorithm is

subject to the same trade-off between the accuracy and resolution as the conventional Dix differentiation (i.e., the accuracy decreases with the relative time-thickness of the interval).

We tested our inversion method on a synthetic data set generated by ray tracing in a three-layer orthorhombic model with pronounced anisotropy and depth-varying orientation of the vertical symmetry planes. Despite the presence of nonhyperbolic moveout caused by both inhomogeneity and anisotropy, we were able to reconstruct the NMO ellipses on conventional-length spreads with sufficient accuracy. Our modeling shows that moveout for dipping events remains close to hyperbolic on surprisingly long spreads, twice as large as the CMP-reflector distance. In contrast, traveltimes for horizontal events start to deviate noticeably from a hyperbola for offsets exceeding the reflector depth. If non-hyperbolic moveout does cause distortions in the NMO ellipses, it is possible to obtain a more reliable estimate of the NMO velocity by using a *nonhyperbolic* moveout equation (Tsvankin and Thomsen, 1994; Grechka and Tsvankin, 1997). On the other hand, it may be possible to include nonhyperbolic moveout in the inversion for the medium parameters.

### Acknowledgments

We are grateful to members of A(nisotropy)-team of the Center for Wave Phenomena (CWP), Colorado School of Mines, for helpful discussions.

### References

- Alkhalifah, T., and Tsvankin, I., 1995, Velocity analysis in transversely isotropic media: *Geophysics*, **60**, 1550–1566.
- Grechka, V., and Tsvankin, I., 1996, 3-D description of normal moveout in anisotropic media, *Geophysics*, submitted (CWP-225).
- Grechka, V., and Tsvankin, I., 1997, Feasibility of non-hyperbolic moveout inversion in transversely isotropic media: *Geophysics*, submitted (CWP-212).
- Grechka, V., Tsvankin, I., and Cohen, J.K., 1997, Normal-moveout velocity and generalized Dix equation for inhomogeneous anisotropic media, *CWP-241*.
- Hubral, P., and Krey, T., 1980, Interval Velocities from Seismic Reflection Measurements: *Soc. Expl. Geophys.*
- Ikelle, L.T., 1996, Anisotropic migration-velocity based on inversion of common azimuthal sections: *J. Geophys. Res.*, **101**, No. B10, 22,461–22,484.
- Sayers, C.M., 1995, Reflection moveout in azimuthally anisotropic media: 65th Ann. Internat. Mtg., Soc. Expl. Geophys., Expanded Abstracts, 340–343.
- Schoenberg, M., and Helbig, K., 1997, Orthorhombic media: Modeling elastic wave behavior in a vertically fractured earth: *Geophysics*, in print.
- Thomsen, L., 1986, Weak elastic anisotropy: *Geophysics*, **51**, 1954–1966.
- Tsvankin, I., 1995, Normal moveout from dipping reflectors in anisotropic media: *Geophysics*, **60**, 268–284.
- Tsvankin, I., 1996a, *P*-wave signatures and notation for transversely isotropic media: An overview: *Geophysics*, **61**, 467–483.
- Tsvankin, I., 1996b, Effective parameters and *P*-wave velocity for azimuthally anisotropic media: 66th Ann. Internat. Mtg., Soc. Expl. Geophys., Expanded Abstracts.
- Tsvankin, I., and Thomsen, L., 1994, Nonhyperbolic reflection moveout in anisotropic media: *Geophysics*, **59**, 1290–1304.
- Wild, P., and Crampin, S., 1991, The range of effects of azimuthal isotropy and EDA anisotropy in sedimentary basins: *Geophys. J. Int.*, **107**, 513–529.

### APPENDIX A: Weak-anisotropy approximation for *P*-wave NMO velocity in an orthorhombic layer

Here, we derive the weak-anisotropy approximation for *P*-wave normal-moveout velocity by linearizing the exact NMO equation (18) in the anisotropic coefficients. The linearized expression for the vertical slowness  $q$ , obtained from the Christoffel equation, is given in the main text [equation (20)]. Differentiating equation (20) with respect to  $p_1$  and  $p_2$ , substituting the results into equation (18) and further linearizing the NMO equation in the coefficients  $\eta^{(1,2,3)}$  yields (we used Mathematica software)

$$\begin{aligned}
 V_{\text{nmo}}^{-2}(\alpha, p_1, p_2) = & \cos^2 \alpha \left\{ [V_{\text{nmo}}^{(2)}]^{-2} - p_1^2 + \sum_{i=1}^3 d_{1i} \eta^{(i)} \right\} \\
 & + 2 \sin \alpha \cos \alpha \left\{ -p_1 p_2 + \sum_{i=1}^3 d_{2i} \eta^{(i)} \right\} \\
 & + \sin^2 \alpha \left\{ [V_{\text{nmo}}^{(1)}]^{-2} - p_2^2 + \sum_{i=1}^3 d_{3i} \eta^{(i)} \right\}, \tag{A1}
 \end{aligned}$$

where  $\eta^{(i)}$  are the linearized anisotropic coefficients from equations (21) – (24), and  $d_{ki}$  are given by

$$d_{11} = -2p_2^2 (1 - 4p_1^2 \tilde{V}^2) (1 - p_1^2 \tilde{V}^2 - p_2^2 \tilde{V}^2), \tag{A2}$$



$$d_{12} = -2(6p_1^2 + p_2^2 - 9p_1^4 \tilde{V}^2 - 5p_1^2 p_2^2 \tilde{V}^2 + 4p_1^6 \tilde{V}^4 + 4p_1^4 p_2^2 \tilde{V}^4), \quad (\text{A3})$$

$$d_{13} = 2p_2^2 (1 - 5p_1^2 \tilde{V}^2 + 4p_1^4 \tilde{V}^4), \quad (\text{A4})$$

$$d_{21} = -4p_1 p_2 (1 - 2p_2^2 \tilde{V}^2) (1 - p_1^2 \tilde{V}^2 - p_2^2 \tilde{V}^2), \quad (\text{A5})$$

$$d_{22} = -4p_1 p_2 (1 - 2p_1^2 \tilde{V}^2) (1 - p_1^2 \tilde{V}^2 - p_2^2 \tilde{V}^2), \quad (\text{A6})$$

$$d_{23} = 4p_1 p_2 (1 - p_1^2 \tilde{V}^2 - p_2^2 \tilde{V}^2 - 2p_1^2 p_2^2 \tilde{V}^4), \quad (\text{A7})$$

$$d_{31} = -2(6p_2^2 + p_1^2 - 9p_2^4 \tilde{V}^2 - 5p_1^2 p_2^2 \tilde{V}^2 + 4p_2^6 \tilde{V}^4 + 4p_1^2 p_2^4 \tilde{V}^4), \quad (\text{A8})$$

$$d_{32} = -2p_1^2 (1 - 4p_2^2 \tilde{V}^2) (1 - p_1^2 \tilde{V}^2 - p_2^2 \tilde{V}^2), \quad (\text{A9})$$

$$d_{33} = 2p_1^2 (1 - 5p_2^2 \tilde{V}^2 + 4p_2^4 \tilde{V}^4). \quad (\text{A10})$$

The parameter  $\tilde{V}$  is defined as

$$\tilde{V} = \frac{1}{2} (V_{\text{nmo}}^{(1)} + V_{\text{nmo}}^{(2)}), \quad (\text{A11})$$

where  $V_{\text{nmo}}^{(1,2)}$  are the semi-axes of the NMO ellipse from the horizontal reflector linearized in the anisotropic coefficients  $\delta^{(i)}$  [equations (15)]:

$$V_{\text{nmo}}^{(i)} = V_{P0} \sqrt{1 + 2\delta^{(i)}} \approx V_{P0} (1 + \delta^{(i)}), \quad (\text{A12})$$

$$(i = 1, 2).$$

There is some flexibility in choosing the parameter  $\tilde{V}$  which reduces to  $V_{P0}$  for isotropic media. Note that  $\tilde{V}$  appears only in equations (A2) – (A10) for the coefficients  $d_{ki}$  that are multiplied by the small quantities  $\eta^{(i)}$  in equation (A1). Therefore, in the linearized weak-anisotropy approximation we can add any anisotropic terms to  $\tilde{V}$  without changing the final result:

$$\tilde{V} = V_{P0} [1 + f(\epsilon^{(i)}, \delta^{(i)}, \eta^{(i)})], \quad (\text{A13})$$

where  $f(\epsilon^{(i)}, \delta^{(i)}, \eta^{(i)})$  is an arbitrary combination of the anisotropic coefficients that goes to zero in isotropic media. Our choice of  $\tilde{V}$  emphasizes the fact that the linearized NMO equation can be represented as a function of just five medium parameters [ $V_{\text{nmo}}^{(1,2)}$  and  $\eta^{(1,2,3)}$ ], while the individual values of the  $\epsilon$  and  $\delta$  coefficients influence only quadratic and higher-order terms.

## APPENDIX B: Effective NMO velocity near intersections of interval NMO ellipses

As emphasized by Grechka et al. (1997) in their discussion of the generalized Dix equation (30), the averaging of the matrices  $\mathbf{W}$  responsible for NMO ellipses is different from the conventional rms averaging of NMO velocities measured in a certain azimuthal direction. In this Appendix we illustrate this difference by examining the effective normal-moveout velocity near intersections of interval NMO ellipses.

Let us consider a two-layer model with intersecting NMO-velocity ellipses [see equation (10)]

$$V_{\text{nmo},i}^{-2}(\alpha) = W_{11,i} \cos^2 \alpha + 2W_{12,i} \sin \alpha \cos \alpha + W_{22,i} \sin^2 \alpha, \quad (i = 1, 2) \quad (\text{B1})$$

and the corresponding effective ellipse [equation (30)]

$$\mathbf{U}^{-1} = \frac{1}{\tau_1 + \tau_2} (\tau_1 \mathbf{W}_1^{-1} + \tau_2 \mathbf{W}_2^{-1}), \quad (\text{B2})$$

where  $\tau_1$  and  $\tau_2$  are interval zero-offset traveltimes. Without loss of generality we can assume that the coordinate system has been chosen in such a way that the ellipses (B1) intersect (or touch) each other at azimuth  $\alpha = 0$ , which implies that

$$W_{11,1} = W_{11,2} = W_{11}. \quad (\text{B3})$$

Evidently, conventional rms averaging of NMO velocities at  $\alpha = 0$  yields the effective velocity

$$V_{\text{rms,eff}}^2(0) = \frac{1}{W_{11}}. \quad (\text{B4})$$

Here, we compare  $V_{\text{rms,eff}}(0)$  with the exact effective NMO velocity in the same direction ( $\alpha = 0$ ) that can be obtained from equation (B2) as

$$V_{\text{ex,eff}}^2(0) = \frac{1}{U_{11}}. \quad (\text{B5})$$

Substituting equations (B1) into equation (B2), we find

$$\frac{V_{\text{ex,eff}}^2(0)}{V_{\text{rms,eff}}^2(0)} - 1 = \frac{\tau_1 \tau_2 (W_{12,1} - W_{12,2})^2}{(\tau_1 + \tau_2) (\tau_1 \det \mathbf{W}_2 + \tau_2 \det \mathbf{W}_1)}. \quad (\text{B6})$$

Since the interval matrices  $\mathbf{W}_i$  are positive definite (Grechka and Tsvankin, 1996), both determinants in the denominator are positive, and the right-hand side of equation (B6) is non-negative. Hence,

$$V_{\text{ex,eff}}(0) \geq V_{\text{rms,eff}}(0), \quad (\text{B7})$$

i.e., the rms averaging of the interval NMO velocities *always* underestimates the effective velocity at an intersection of the NMO ellipses.

As a simple example, let us consider a model that consists of two identical horizontal orthorhombic layers with interchanged vertical symmetry planes. The interval ellipses (solid and dashed lines) in such a model are identical, but rotated with respect to each other by  $90^\circ$  (Figure B1). The effective NMO ellipse (dotted line in Figure B1) in this case is a *circle* because the effective NMO velocities in both symmetry planes coincide with each other. Clearly, in some vicinity of the azimuth  $\alpha = \pi/4$  the effective NMO velocity is *greater* than both interval velocities. At the azimuth  $\alpha = \pi/4$ , two interval NMO velocities and the rms-averaged value are equal, and [see equation (B4)]:

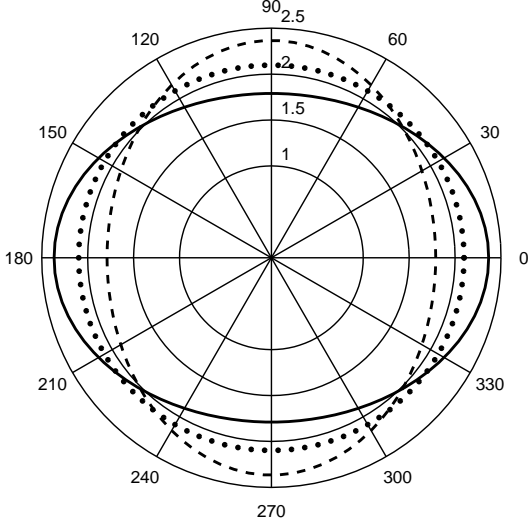


**Figure B1.** The interval  $P$ -wave NMO ellipses (solid and dashed) and the effective NMO ellipse (dotted) in a two-layer orthorhombic model. Both layers are horizontal, have the same thickness  $z_1 = z_2 = 1.0$  km and the same elastic parameters, but their vertical symmetry planes are rotated by  $90^\circ$  with respect to each other. The vertical velocity  $V_{P0,1} = V_{P0,2} = 2.0$  km/s. The parameters  $\delta$  that control the NMO velocity in the symmetry planes are interchanged:  $\delta_1^{(1)} = -0.1$ ,  $\delta_1^{(2)} = 0.2$ , and  $\delta_2^{(1)} = 0.2$ ,  $\delta_2^{(2)} = -0.1$ .

$$\frac{1}{V_{\text{rms,eff}}^2(\pi/4)} = \frac{1}{2} \left( \frac{1}{[V_{\text{nmo}}^{(1)}]^2} + \frac{1}{[V_{\text{nmo}}^{(2)}]^2} \right), \quad (\text{B8})$$

where  $V_{\text{nmo}}^{(i)}$  are the interval NMO velocities in the symmetry planes. Therefore, the squared rms velocity at  $\alpha = \pi/4$  represents the *harmonic* average of the squared semi-axes of the interval NMO ellipse.

Since the exact effective NMO velocity in this model is circular, at  $\alpha = \pi/4$  it is equal to the values at the symmetry planes ( $\alpha = 0$  or  $\alpha = \pi/2$ ), which can be found by conventional rms averaging (see Grechka et al., 1997):

$$V_{\text{ex,eff}}^2(\pi/4) = \frac{1}{2} \left( [V_{\text{nmo}}^{(1)}]^2 + [V_{\text{nmo}}^{(2)}]^2 \right). \quad (\text{B9})$$

Thus, the exact squared NMO velocity  $V_{\text{ex,eff}}^2(\pi/4)$  is the *arithmetic* average of  $[V_{\text{nmo}}^{(1)}]^2$  and  $[V_{\text{nmo}}^{(2)}]^2$ . According to the relation between the harmonic and arithmetic averages,

$$V_{\text{ex,eff}}(\pi/4) \geq V_{\text{rms,int}}(\pi/4), \quad (\text{B10})$$

in agreement with equation (B6).